JOURNAL OF GEOPHYSICAL RESEARCH, VOL. 86, NO. C10, PAGES 9929-9938, OCTOBER 20, 1981

Simulation of the Effects of Surface Fluxes of Heat and Moisture in a Mesoscale Numerical Model 1. Soil Layer

MICHAEL C. MCCUMBER AND ROGER A. PIELKE

Department of Environmental Sciences, University of Virginia, Charlottesville, Virginia 22903

A parameterization for bare soil is developed, which is to be incorporated in a mesoscale numerical prediction model. This parameterization is generalized to accomodate 11 types of soil in addition to peat, using mean soil characteristics. The sensitivity of the scheme to several soil parameters is evaluated by a series of one-dimensional simulations. It is shown that the most important soil characteristic is the soil moisture, which regulates the strength of the heat fluxes between the atmosphere and the ground.

1. INTRODUCTION

Much attention is devoted to the parameterization of the boundary layer in atmospheric numerical prediction models [*Pielke,* 1974; *Anthes and Warner,* 1978; *Deardorff,* 1974; *Tapp and White,* 1976], but less regard is given to the boundary itself—the surface of the earth. While many models employ a surface energy budget to predict the surface soil temperature, the treatment of soil moisture remains very crude, in general [*Pielke,* 1974; *Carpenter,* 1979; *Burk,* 1977; *Perkey,* 1976].

A detailed mathematical model for predicting soil temperature and soil moisture was first proposed by *Philip* [1957], but it was only recently coupled with a predictive atmospheric model [*Sasamori,* 1970; *Zdunkowski et al.,* 1975]. Unfortunately, advective effects were ignored since these studies were limited to one dimension. However, in a recent work, *Garrett* [1978] extended Sasamori's work to three dimensions.

The intent of the present study is to estimate the importance of properly simulating the ground surface in a mesoscale model by examining the relationship between an evolving sea breeze circulation in south Florida and the underlying ground surface. This is accomplished by coupling an atmospheric prediction model with a multi-level soil layer. Temperature and moisture budgets are computed for the soil layer, which is generalized to accomodate as many as 11 types of soil in addition to peat.

This paper is the first of three parts, which comprise the experiment. A parameterization for bare soil is discussed here. Tests are presented, using generalized native south Florida soils, with two purposes in mind. The first purpose is to examine the sensitivity of the parameterization to the initialization of some soil characteristics (e.g., albedo, surface wetness). The second purpose is to establish a benchmark behavior for each soil: These behaviors are important in the analyses presented in the next two papers.

The second paper in ths series presents and evaluates a vegetation parameterization [*Deardorff,* 1978], while several three-dimensional numerical simulations for south Florida are analyzed in the last paper. The latter simulations are designed to investigate the effect on the sea breezes of increased surface complexity, as well as the feedback from the atmosphere to the soil. The results are influenced by local effects, which arise from the characteristics of the individual soils, and regional effects, which originate from horizontal heterogeneity of the land surface.

2. THE NUMERICAL MODELS

The Atmospheric Model

The University of Virginia Mesoscale Model (UVMM) is used to predict the state of the atmosphere. It was developed from the original model of *Pielke* [1974] that was later modified in *Mahrer and Pielke* [1977]. The model is hydrostatic and initially barotropic. Radiation fluxes from the atmosphere are computed and a boundary layer is explicitly defined, which is permitted to grow in response to surface heat fluxes and changes in surface roughness.

The Soil Model

The soil temperature is treated similarly to *Mahrer and Pielke* [1977] where the surface temperature is computed from the surface energy balance equation

$$R_n + \rho L u_* q_* + \rho c_p u_* \theta_* - G = 0 \tag{1}$$

R_n is the net radiation flux at the surface, and the second and third terms are the turbulent latent and sensible heat fluxes, respectively. G is the soil heat flux. The turbulent quantities u_*, θ_*, and q_* are defined as

$$u_* = k_0 (u^2 + v^2)^{0.5} / (\ln (z/z_0) - I_1) \tag{2}$$

$$\theta_* = k_0 (\theta - \theta(z_0)) / (0.74 (\ln (z/z_0) - I_2)) \tag{3}$$

$$q_* = k_0 (q - q(z_0)) / (0.74 (\ln (z/z_0) - I_2)) \tag{4}$$

where k_0 is von Karman's constant (0.35), z is height, and z_0 is a turbulent roughness height. Terms I_1 and I_2 are adjustments based on stability. Equations (2)–(4) represent the turbulent momentum, heat, and moisture at the surface.

Below the soil surface, only vertical diffusion is permitted, using

$$C \frac{\partial T_s}{\partial t} = \frac{\partial H_s}{\partial z} \tag{5}$$

where the vertical soil heat flux

$$H_s = \lambda \frac{\partial T_s}{\partial z}$$

The volumetric heat capacity, C, is simply defined as

$$C = (1 - \eta_s) C_i + \eta \tag{6}$$

Here η is the volumetric moisture content and η_s is the saturation moisture content, which is also the porosity. C_i is the air

Paper number 1C1123.
0148-0227/81/001C-1123$01.00

dry volumetric heat capacity for soil type i. In (6) the heat capacity of air has been omitted since it is negligibly small [*Sellers*, 1965; *De Vries*, 1975].

The thermal conductivity, λ, (cal s^{-1} cm^{-1} $°C^{-1}$) varies over several orders of magnitude as a soil dries out. To account for this, a mean curve was fitted to the data plotted in Figure 4 in *Al Nakshabandi* and *Kohnke* [1965]. Its functional form is

$$\lambda = \exp(-(P_f + 2.7)) \qquad P_f \leq 5.1$$
$$\lambda = 0.00041 \qquad P_f > 5.1 \tag{7}$$

P_f is the base 10 logarithm of the magnitude of the moisture potential, ψ, which is expressed as a head of water (cm). Al Nakshabandi and Kohnke demonstrated that the relationship between thermal conductivity and moisture potential is virtually independent of soil textural class.

The prognostic equation for soil moisture content (η) is

$$\rho_w \frac{\partial \eta}{\partial t} = \frac{\partial W_s}{\partial z} \tag{8}$$

W_s is the moisture flux within the soil (defined as positive downward), ρ_w is the density of liquid water (g cm^{-3}), and z is a vertical coordinate within the soil profile, defined (as it is in the atmosphere) as positive upward.

Equation (8) is less refined than Philip's detailed mathematical model for moisture transfer in the soil, which *Sasamori* [1970] and *Garrett* [1978] used with their atmospheric numerical models. However, since only domain-averaged soil fluxes are desired here and furthermore since detailed soil data are commonly unavailable for either initializing or vertifying a mesoscale numerical model for a specific region (e.g., south Florida), a simpler approach seems to be justified.

The soil moisture flux (which incorporates both the vapor and liquid phases) is defined as

$$W_s = K_\eta \rho_w \frac{\partial(\psi + z)}{\partial z} \tag{9}$$

K_η is the hydraulic conductivity, and ψ is the moisture potential, which represents the work required to extract water from the soil against capillary and adhesive forces. Another form of this equation is

$$W_s = D_\eta \rho_w \frac{\partial \eta}{\partial z} + K_\eta \rho_w \tag{10}$$

noting that the diffusivity is merely

$$D_\eta = K_\eta \frac{\partial \psi}{\partial \eta}$$

The variables K_η, D_η, and ψ are related to η through a set of simple relationships found in *Clapp and Hornberger* [1978]:

$$\psi = \psi_s \left(\frac{\eta_s}{\eta}\right)^b \tag{11}$$

$$K_\eta = K_{\eta_s} \left(\frac{\eta}{\eta_s}\right)^{2b+3} \tag{12}$$

and

$$D_\eta = -\frac{bK_{\eta_s}\psi_s}{\eta}\left(\frac{\eta}{\eta_s}\right)^{b+3} \tag{13}$$

Subscript s refers to saturation. The exponent b is a function of the USDA soil textural class [*U.S. Department of Agriculture* (USDA), 1951], as are ψ_s, K_{η_s}, and η_s. Clapp and Hornberger provide a table of mean values for each of these four parameters as they are applied to 11 soil classes. Data for the native south Florida soils used in this study are reproduced in Table 1. Values for peat are a composite of mean observed data [*Rijtema*, 1970] and fitted data (to permit the use of equations (11)–(13)).

TABLE Soil Parameters for Three USDA Textural Classes [*USDA*, 1951] Plus Peat

Soil Type	η_s	ψ_s	K_{η_s}	b	η_{wilt}	c_i
Sand	0.395	−12.1	0.01760	4.05	0.0677	0.350
Sandy Loam	0.435	−21.8	0.00341	4.90	0.1142	0.321
Sandy Clay	0.426	−15.3	0.00022	10.40	0.2193	0.281
Peat	0.863	−35.6	0.00080	7.75	0.3947	0.200

Units for soil porosity (η_s) are cm^3 cm^{-3}, saturation moisture potential (ψ_s) is given in cm, and the saturation hydraulic conductivity (K_{η_s}) is expressed in cm s^{-1}. Exponent b is dimensionless. Permanent wilting moisture content (η_{wilt}) is in cm^3 cm^{-3}, and the dry volumetric heat capacity (c_i) is in cal cm^{-1} $°C^{-1}$. The first four variables are reproduced from *Clapp and Hornberger* [1978], with permission.

Heat capacities for air dry soils were calculated from a few known values for sand, clay, loam, and peat, using the percentage weight compositions of *Petersen et al.* [1968]. Permanent wilting moisture contents were computed assuming a moisture potential of −15,300 cm (i.e., 15 bar).

Usually the transfer of moisture between the soil and the atmosphere occurs as water vapor. The surface moisture potential, which is a measure of the soil wetness, is related to water vapor at equilibrium by the relative humidity [*Philip*, 1957; *Edlefsen and Anderson*, 1943]

$$h = \exp - \left[\frac{g\psi_G}{R_v T_G}\right] \tag{14}$$

The atmospheric moisture variable, the specific humidity, is then determined from

$$q_G = hq_s \tag{15}$$

The saturation specific humidity is written as

$$q_s = 0.622 \left[\frac{e_s}{p - 0.378\, e_s}\right] \tag{16}$$

and the saturation vapor pressure (mbar) is only a function of the surface temperature

$$e_s = 6.1078 \exp\left[(17.269)\frac{T_G - 273.16}{T_G - 35.86}\right] \tag{17}$$

The degree of wetness of the soil also affects the radiation balance at the surface by altering the surface albedo, which is lower for wetter than drier soils. From *Idso et al.* [1975], the albedo is expressed as a function of soil wetness.

$$a_s = 0.31 - 0.34\,\Delta \qquad \Delta \leq 0.5$$
$$a_s = 0.14 \qquad \Delta > 0.5 \tag{18}$$

where $\Delta = (\eta/\eta_s)$ is the fractional wetness of the soil. Although Idso presents relationships for only Avondale loam, (18) is extended to other classes as a reasonable first-order estimate. Limiting albedos for Florida peat are known [*Gannon*, 1978],

TABLE 2. Initial Atmospheric Profile

Height, m	θ, K	q, g g^{-1}	Wind speed, m s^{-1}	Direction, deg
6000	326.2	0.0030	4.72	58
5000	323.5	0.0035	2.24	63
4000	318.9	0.0026	2.80	90
3000	313.5	0.0054	4.00	90
2000	308.5	0.0076	4.00	90
1200	305.0	0.0092	4.57	110
700	301.5	0.0145	6.00	110
300	300.0	0.0165	6.04	94
100	299.8	0.0187	5.65	93
50	299.7	0.0189	5.40	93
25	299.6	0.0190	5.15	93

so that the appropriate linear relationships for peat are

$$a_s = 0.14\,(1 - \Delta) \qquad \Delta \le 0.5$$

$$a_s = 0.07 \qquad \Delta > 0.5 \tag{19}$$

The total surface albedo is determined from

$$a_G = a_s + a_n \tag{20}$$

where a_n is an adjustment to take into account the effect of the solar zenith angle

$$a_n = 0.01\,(\exp\,(aZ^{1.5}) - 1)$$

The zenith angle is Z and $a = 0.003286$. This equation is a fit to the normalizing function of *Idso et al.* [1975].

3. Numerical Procedures

Horizontal advection in the atmospheric model employs an upstream interpolated cubic spline [*Mahrer and Pielke,* 1978]. This scheme is very accurate since it preserves phase and amplitude very well. No horizontal transfer of heat or moisture is assumed in the soil layer.

Vertical diffusion in the atmosphere and the soil is accomplished by using a generalized version of the Crank-Nicolson scheme [*Paegle et al.,* 1976]. No horizontal diffusion is parameterized, although a discriminating low pass filter [*Mahrer and Pielke,* 1978] is applied in the horizontal to the prognostic atmospheric variables (i.e., u, v, θ, and q).

The Newton-Raphson iterative algorithm is used to solve for the surface soil temperature, which occurs as a fourth power component of the net radiation term in the surface energy budget (equation (1)).

And last, the soil-atmosphere system is closed by demanding continuity of mass across the air-soil interface [*Sasamori,* 1970], stated mathematically as

$$W_a - (W_s)_G = 0 \tag{21}$$

where W_a is the turbulent atmospheric moisture flux at the surface, defined as

$$W_a = \rho u_* q_*$$

Here ρ is the air density. $(W_s)_G$ is the soil moisture flux at the surface. At each time step, $(W_s)_G$ is initially estimated from (10). Thereafter it is weighted by

$$(W_s)_G^{n+1} = \delta(W_s)_G^n + (1 - \delta)W_a \qquad 0 \le \delta \le 1 \tag{22}$$

Here δ is an empirically derived weighting factor. Superscript n refers to the iteration of a guess value. The purpose of (22) is to hasten the rate at which the atmospheric and soil moisture fluxes converge.

Once updated, the soil moisture flux is used to update the surface moisture potential

$$\psi_G = \psi_{G-1} + (z_G - z_{G-1})\rho_w \left[\frac{(W_s)_G}{(K_\eta)_G} - 1\right] \tag{23}$$

Subscript G refers to the ground surface and G-1 refers to the next lower soil level. Note that (23) is just a reorganization and a finite difference representation of (9).

The new value for ψ_G is used to update η and then K_η and D_η at the surface (equations (11)–(13)).

The moisture fluxes are assumed to have converged [*Garrett,* 1978] when

$$\left|\frac{W_a - (W_s)_G}{W_a}\right| < 0.001$$

The fastest convergence of the moisture fluxes is ensured when the weighting factor $\delta > 0.5$. When the soil becomes fairly dry (e.g., $h < 0.70$) experience has shown that it is necessary to skew δ strongly toward 1.0 to assure convergence.

4. Initial and Boundary Conditions

At the ground, a no-slip boundary condition is applied to the velocity components, while the surface temperature and specific humidity are predicted. The horizontal components of velocity, the potential temperature, and the specific humidity are all specified as constants at the model top.

The atmospheric and soil grids expand in the vertical dimension. The smaller grid increments are situated near the ground surface, where the largest temperature and moisture gradients exist. Grid increments scale upward from 25 m to 1 km in the atmosphere and from 0.5 to 21 cm in the soil. This results in 11 levels in an atmosphere 6 km deep and a 1 m soil profile with 14 levels.

The initial profiles of the atmospheric variables are given in Table 2. Some of the constants used to initialize the model are listed in Table 3. The starting soil surface temperature is obtained by descending dry adiabatically from the first grid level in the atmosphere. Then the other soil temperatures are defined as departures from the surface value.

The soil moisture profile is generated in a similar way, except that the surface moisture is initially assigned. The type of soil is also assigned.

All simulations are commenced at sunrise. The synoptic scale winds are assumed to be geostrophic above the initial height of the boundary layer (600 m). Within the boundary layer, a balance is prescribed between the pressure gradient, coriolis force, and the friction force.

5. Results of Sensitivity Tests

Numerous one-dimensional simulations were run to investigate the sensitivity of the soil parameterization to several soil

TABLE 3. Some Constants Used to Initialize the Model

	Parameters
Surface pressure	1018 mbar
Surface specific humidity (q_G)	0.019 g g^{-1}
Geostrophic wind	6 m s^{-1} from 110° (east)
Initial height of planetary boundary layer	600 m
Roughness length over land (z_0)	4.0 cm

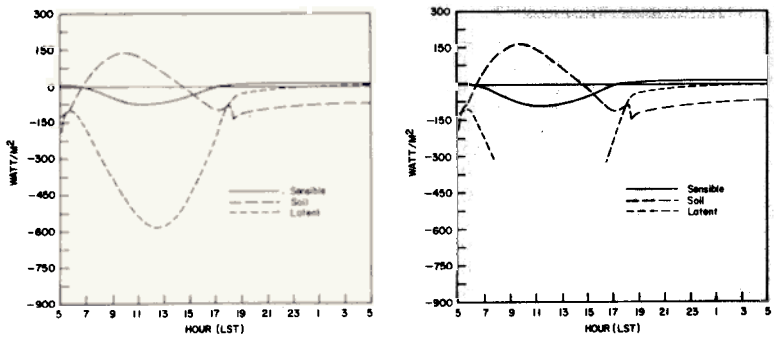

Fig. 1. Effect of albedo on surface heat fluxes for marsh. Initial moisture content is 0.86 cm^3 cm^{-3}. (Left) Albedo is constant (0.20). (Right) Albedo is variable. Fluxes directed toward the atmosphere are negative.

characteristics. This is very important because sampled soil data are commonly unavailable at sites that are selected for simulation (e.g., south Florida). Hence, proper initialization is difficult.

One recourse is to use available soil temperature and moisture profiles, which were sampled at some other location, such as O'Neill, Nebraska [*Lettau and Davidson,* 1957]. However, caution must be observed since there may be a substantial difference in the soil types and even the soil conditions between the sampled site and the region to be simulated. For this reason, a better approach is to define the initial soil profiles for a simulation in terms of departures from the surface temperature and moisture, which can be estimated. It is also common practice to assume that the ground is horizontally homogeneous. However, where soil variability is important, soil temperature and moisture profiles must be specified for each type of soil represented.

Effect of Surface Albedo and Surface Moisture

Five soils, which are representative of native south Florida soils, were tested: sand, sandy loam, sandy clay, peat, and marsh (i.e., saturated peat). Although peat is not truly a soil, it will be treated as such for the purposes of this discussion.

A 24 hour simulation was run for each type of soil for each of two cases: (1) the albedo was set to 0.20 and held constant, and (2) the albedo was free to vary as a function of the surface moisture content (equations (18) and (19)). Energy fluxes for marsh and sand are depicted in Figures 1 and 2 since they represent the wet and dry extremes. Their mid-day albedos were 0.07 and 0.29, respectively. In each instance, there is some modification in the strength of the fluxes, but the basic shape of the plots (i.e., the temporal response) is essentially unaltered. The loam and the clay behaved similarly.

The net effect of the constant albedo was to cool the marsh by 1°C and warm the sand by 2.5°C. Smaller changes were found for clay and loam (0.6°C or less).

Sensitivity of the soil parameterization to the initial soil moisture content was also evaluated for the same five soil types. Time series plots of energy fluxes (W m^{-2}) are presented in Figure 3 for sand. These plots are representative of the response of all soils tested. In Figure 3 the initial moisture content for the wetter sand is 0.12 cm^3 cm^{-3}, whereas it is 0.07 cm^3 cm^{-3} for the drier sand. Soil albedos were fixed at 0.20, and the initial soil moisture profile was assumed to be vertically homogeneous.

When the moisture supply was plentiful, a substantial fraction of the available surface energy was used for evaporation. This meant that less energy was available to warm the soil, which resulted in a cooler soil and a weaker sensible heat flux. The lower surface temperature in turn produced a smaller surface temperature gradient, which resulted in a diminished soil heat flux, even though the thermal conductivities were much larger for the moist sand (equation (7)).

In the dry sand, the surface moisture was quickly depleted. This caused a sharp drop in the surface relative humidity and the surface specific humidity (Figure 4). The attendant reduction in the latent heat flux was accompanied by a stronger sensible heat flux that promoted deeper turbulent transfer in the atmosphere.

Energy diverted from evaporation was principally used to warm the soil and air. For example, the temperature increase for the dry sand is 3 times that of the moist sand. As a result, the soil heat flux doubled, and the sensible heat flux nearly quadrupled.

Note that the sensible heat flux is approximately symmetric about local noon for both simulations, while the latent heat flux is similarly symmetric for only the wetter sand in Figure

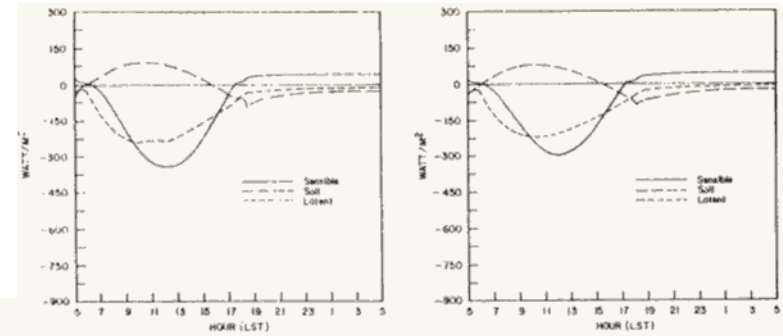

Fig. 2. Same as Figure 1, except for sandy soil. The initial moisture content is 0.07 cm^3 cm^{-3}.

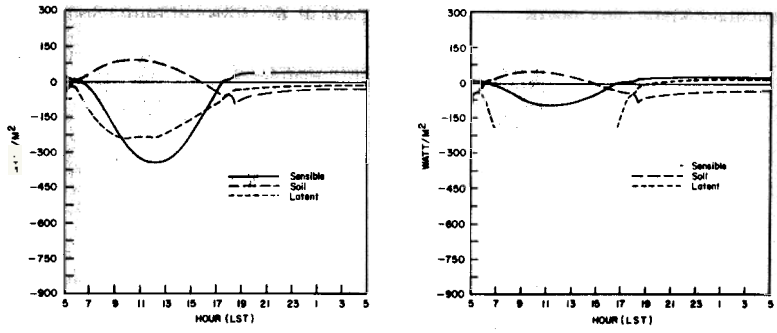

Fig. 3. Effect of initial soil moisture for sand with a constant albedo (0.20). (Left) Initial moisture content is 0.07 cm^3 cm^{-3}. (Right) Initial moisture content is 0.12 cm^3 cm^{-3}.

3. This is a consequence of the low soil relative humidity for the dry sand (Figure 4), which diminishes the magnitude of the surface specific humidity by virtue of (15). For this reason, the latent heat flux peaks near 1000 LST, about 2 hours prior to the maximum sensible heat flux. When the soil relative humidity is high (Figure 5), q_G varies in phase with q_s, which is strongly influenced by the surface soil temperature. In this case, both the sensible and latent heat fluxes peak near 1200 LST.

Within 1 or 2 hours prior to sunset, a surface inversion forms in the atmosphere, capping the region of turbulent transfer. Evaporation from the ground continues to export moisture to the atmosphere where it accumulates in the lowest 200 m, thereby reversing the moisture flux divergence which prevailed during most of the afternoon. This is evidenced by a second maximum in the surface specific humidity, principally between 1700 and 1800 LST (Figures 4 and 5). A similar increase occurs in the atmospheric specific humidity near the ground (not shown). This phenomenon is supported observationally [*Geiger*, 1965, pp. 105–107].

Influence of Initial Soil Temperature and Moisture Profiles

It is acknowledged that vertical gradients in soil moisture and soil temperature, which in effect drive the soil moisture and heat fluxes, may be as important as the surface values of these parameters. Therefore, vertical gradients for both quantities were tested for a sandy soil (sand was selected since it is the most abundant south Florida soil).

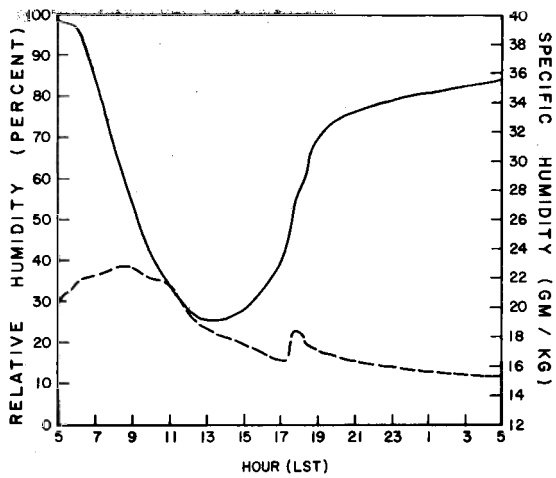

Fig. 4. Diurnal variation of specific humidity (dashed) and relative humidity (solid) at the surface of sandy soil. Initial moisture content is 0.07 cm^3 cm^{-3}. The abrupt rise in specific humidity accompanied the development of a surface inversion near sunset.

Table 4 lists the seven simulations in which either temperature or moisture gradients varied from a base (or reference) state. Data for the base state (Table 5) is secured from a morning observation taken from Lettau and Davidson.

The variations in gradients included a linear increase with depth, a linear decrease with depth, and zero vertical gradient. The temperature gradients were ±4 K m^{-1}, while the moisture gradients were 0.20 cm^3 cm^{-3} m^{-1} and −0.07 cm^3 cm^{-3} m^{-1}. All runs commenced at sunrise and integrated for 12 hours. The initial surface moisture content and surface temperature were identical in each simulation. The results are summarized in Table 6.

For a given moisture content and soil type, the temperature profile that developed is essentially independent of the particular initialization chosen. This means that solar forcing, which is quite strong, is clearly the dominant influence upon the soil temperature. The initialization chosen for the soil temperature may be more critical, however, should the integration commence at night or should the sky be cloudy.

On the other hand, varying the initial profile of soil moisture content had a considerably greater impact than did varying the temperature profile. This indicates that the results are dominated by the moisture initialization. There is no easy answer as to how the soil moisture should be initialized when observed on-site data are unavailable. Therefore, it is assumed that the soil moisture is vertically homogeneous in all subsequent simulations in this study. The temperature field will be initialized with the profile in Table 5.

Effect of Soil Type

Three experiments were performed to test each of the four soil classes used in this study: sand, sandy clay, sandy loam,

TABLE 4. Tests to Determine the Influence of the Initial Temperature and Moisture Profiles in the Soil

	$\frac{\partial T_s}{\partial z}$	$\frac{\partial \eta}{\partial z}$
Experiment		
1	O'Neill, Neb.	O'Neill, Neb.
2	0	O'Neill, Neb.
3	4.0 K m^{-1}	O'Neill, Neb.
4	−4.0 K m^{-1}	O'Neill, Neb.
5	O'Neill, Neb.	0
6	O'Neill, Neb.	0.20 cm^3 cm^{-3} m^{-1}
7	O'Neill, Neb.	−0.07 cm^3 cm^{-3} m^{-1}
Initial surface moisture (all cases)		0.12 cm^3 cm^{-3}

TABLE 5. O'Neill, Nebraska, Base State Data for the Soil Layer [*Lettau and Davidson*, 1957].

Depth, cm	T_s, K	η, cm^3 cm^{-3}
0.0		0.120
0.5		0.120
1.5		0.117
3.0		0.109
5.0		0.093
8.0		0.086
12.0		0.083
18.0		0.083
26.0		0.083
36.0		0.083
48.0		0.083
62.0		0.083
79.0		0.083
100.0		0.083

TABLE 6. Effect of Initial Soil Temperature and Moisture Profiles

	Variable Temperature	Variable Moisture
ΔT_G, °C	0.3	3.7
Δq_G, g kg^{-1}	0.1	4.1
ΔLE, W m^{-2}	5.0	110.0
ΔH, W m^{-2}	5.0	75.0

The first column refers to a set of experiments in which the temperature profile was varied from a base state while the moisture profile was unchanged. The second column refers to another set of experiments where the moisture profile varied while the temperature profile was fixed. The values represent the maximum range for each set of experiments for the surface temperature (T_G), surface specific humidity (q_G), latent heat flux (LE) and sensible heat flux (H).

and peat. Aside from differences in soil properties (e.g., thermal and moisture conductivities, heat capacities, etc.), the experiments differed only in the initialization of the surface moisture (vertical homogeneity is assumed).

The experiments are (A) $\eta = 0.75\ \eta_s$, (B) $\psi = -5000$ cm, and (C) $\psi = -15{,}300$ cm (i.e., wilting moisture content). Thus the soils progress from wet (A) to dry (C). Surface albedo is constant (0.20).

It is evident from the data in Table 7 (with the exception of peat) that, unlike *Zdunkowski et al.* [1975], the outcome is much more dependent upon the initial moisture (soils are drier from left to right) than upon the type of soil. The same relationship occurs for the surface sensible and latent heat fluxes.

6. Reference Soil Behavior

The native south Florida soils used in this study vary widely in drainage and water retention characteristics. In general, drainage is greatest and water retention least in coarse-grained soils (e.g., sand). Drainage decreases as the texture becomes finer, while water retention increases. However, the available water content (i.e., freely available to plants) decreases when the clay fraction gets large [*Salter and Williams*, 1965; *Jadhav et al.*, 1977].

The data for the simulations in the third paper of this series apply to a midsummer day in south Florida. Since observed soil moisture data are unavailable, moisture contents (cm^3 cm^{-3}) are assigned to each type of soil as the following: 0.07 (sand), 0.17 (sandy loam), 0.27 (sandy clay), 0.58 (peat), and 0.86 (marsh). These values were estimated taking into consideration the differences in drainage and water retention of the soils. The soil moisture for the clay and the loam are mid-range values of available water content corresponding to a moisture potential of −2000 cm.

The diurnal behavior of each soil for 24 hour simulations commencing at sunrise is presented in Figures 6–8. Vertical homogeneity is assumed initially in all soil parameters, except for soil temperature, since the actual profiles are unknown.

It is apparent from the figures that the soil behavior is predominantly determined by the moisture content. For example, consider the sensible heat flux (Figure 7). The heat fluxes for the moist soils, which evaporated moisture at nearly the potential rate (i.e., high surface relative humidity), are similar. However, the dry sand yielded a substantially more vigorous sensible heat flux than the other soils. *Van Bavel and Hillel* [1976] present a similar relationship between soil wetness and the intensity of computed sensible and latent heat fluxes.

There is a somewhat wider disparity between latent heat fluxes. Marsh and peat behaved similarly, as did sandy clay and sandy loam. This is a direct reflection of the control exerted by the surface relative humidity. Since soil temperatures amongst these four soils never ranged more than 3°C, the differentiation in q_G must generally be attributable to the surface relative humidities.

Peat and marsh each evaporated moisture very near the potential rate at all times. But the afternoon relative humidity in the loam dropped to 90% and it fell to 76% for the clay (Table 8). Sand was markedly drier with a relative humidity of only 29%.

Some variability can be attributed to the different soils themselves. For instance, sandy clay warmed by about 2°C more than the sandy loam, yet they were both initialized with the same soil moisture potential. However, the albedo of each soil is determined as a function of the fractional wetness of the soil, so that the albedos are never the same. In Table 8, the surface albedo for the clay is 18.2%, while it is 25.4% for the loam.

TABLE 7. Evaluation of the Effect of Soil Type

	Maximum Soil Temperature (T_s)			Maximum Atmosphere Potential Temperature (θ)			Total Soil Moisture Extracted		
Soil Type	A	B	C	A	B	C	A	B	C
Sand	307.4	313.7	322.5	302.7	305.0	307.8	7.26	6.14	3.20
Sandy clay	307.7	315.5	322.1	302.7	305.5	307.7	7.17	5.53	3.14
Sandy loam	307.4	312.0	320.3	302.7	304.6	306.8	7.25	6.50	4.04
Peat	307.4	309.2	315.0	302.7	303.4	305.4	7.21	6.88	5.74

The three experiments differ by the initialization of soil moisture. They are (A) $\eta = 0.75\ \eta_s$, (B) $\psi = -5000$ cm, and (C) $\psi = -15300$ cm. Temperatures are given in degrees K and extracted moisture is expressed as a depth of water (mm). Potential temperature is at a height of 37.5 m.

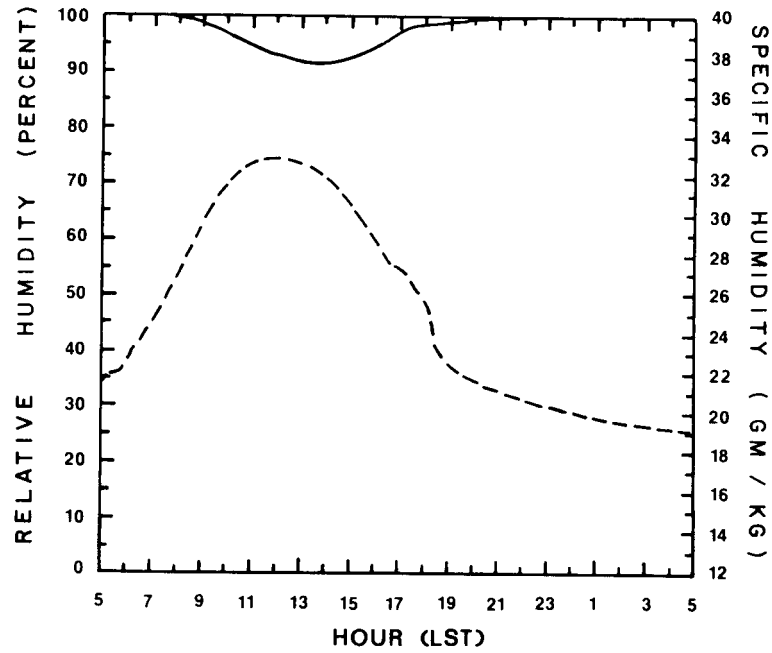

Fig. 5. Same as Figure 4, except the initial moisture content is 0.12 cm^3 cm^{-3}.

Although the soil thermal conductivities and the moisture release characteristics are different for each soil, it appears that the additional net radiation received by the clay (60 W m^{-2} at 1315 LST) accounts for the greater warming.

7. Summary

Soil moisture is a very influential soil variable. The degree of wetness of the soil affects the albedo, which in turn regulates the receipt of solar energy. Relative humidity at the soil surface, itself a function of soil moisture, determines the partitioning of surface energy into sensible and latent heat. Even the soil heat flux is influenced by wetness, since the thermal conductivity is closely related to moisture potential.

Numerical experiments support the findings of *Gannon* [1978] that moisture is the most important soil variable. The effects of surface albedo and soil texture (i.e., type of soil) on heat fluxes at the air-soil interface are much less.

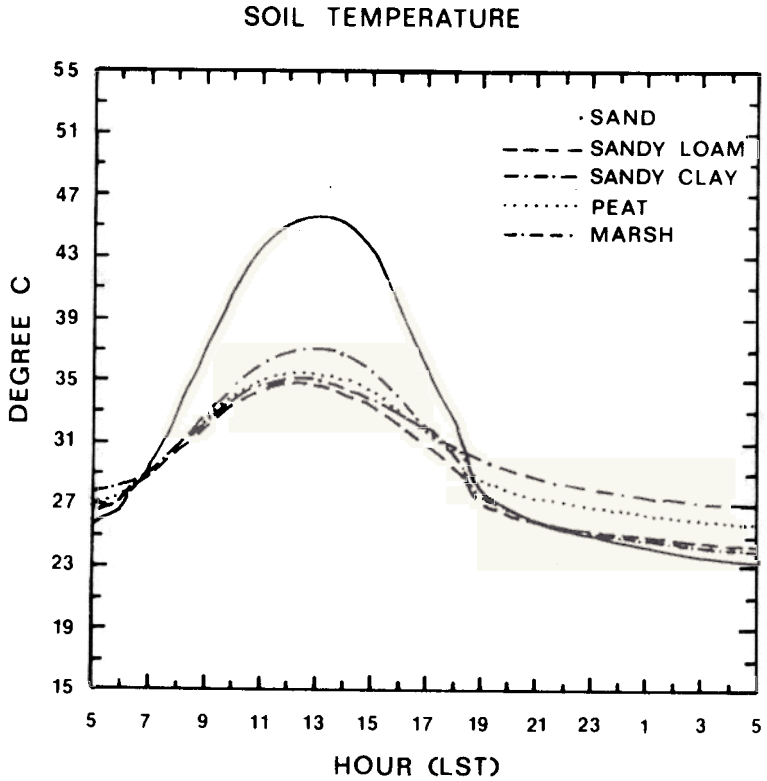

Fig. 6. Predicted soil surface temperature (°C) as a function of native south Florida soil type. Time is in hours Local Standard Time. Notice the smaller diurnal range for the wettest soils (marsh and peat).

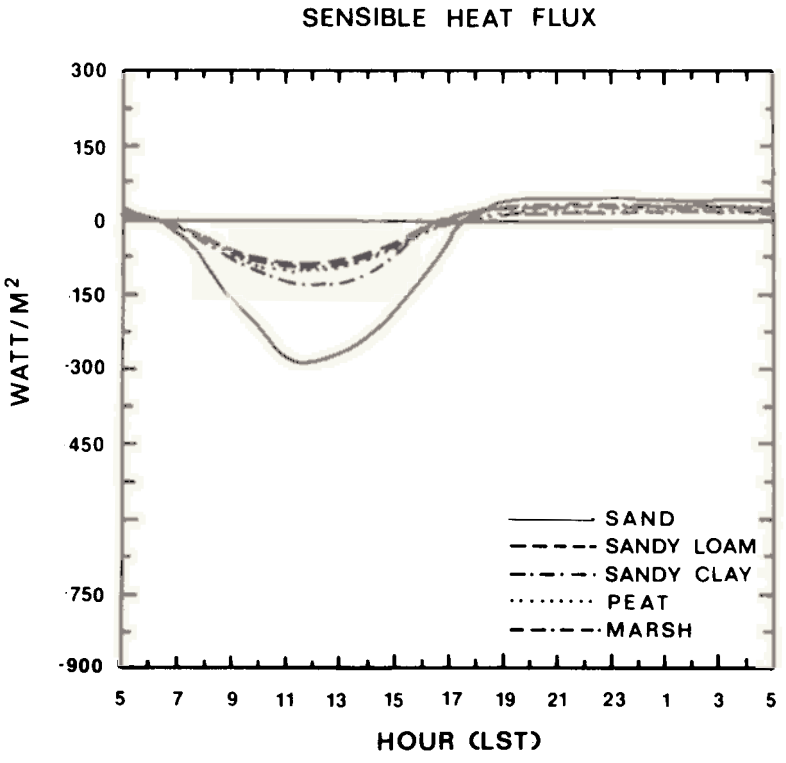

Fig. 7. Predicted sensible heat flux density (W m^{-2}) as a function of soil type. Fluxes directed toward the atmosphere are negative.

Beside the surface moisture content, it is found that the initial vertical profile of moisture is also influential. Surface heat fluxes are more than an order of magnitude more sensitive to the initial moisture profile than to the temperature profile within the soil (this applies to simulations, which begin at sunrise and which assume clear skies throughout the run). This poses a dilemma for the modeller, who is rarely provided with observed data to initialize a soil layer. Vertical homogeneity for the soil moisture is adopted in this paper as a simple, though not a satisfactory, solution to the problem.

Benchmark simulations for three south Florida soils and peat indicate that soil characteristics (e.g., temperature, water

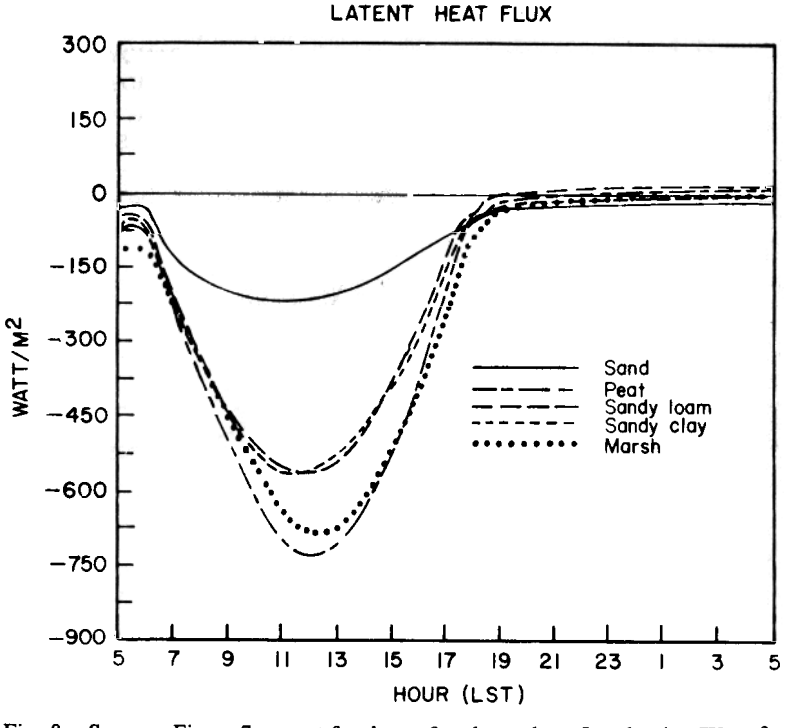

Fig. 8. Same as Figure 7, except for the surface latent heat flux density (W m^{-2}).

TABLE 8. Simulated Surface Condition for Five Soils at 1315 LST

Soil Type	T_G	h	a_G
Sand	319.0	29	0.292
Sandy loam	308.1	90	0.254
Sandy clay	310.5	76	0.182
Peat	308.6	100	0.070
Marsh	308.2	100	0.070

T_G is the soil temperature (K), h is the relative humidity (%), and a_G is the albedo.

vapor flux, etc.) are principally governed by soil wetness. Some variations are due to surface albedo, but the effect of different soil wetness is much more apparent.

Clearly, proper simulation of the ground surface in a numerical, atmospheric model must include the accurate prediction of soil wetness, since this is the soil characteristic which principally determines the phase and the relative strength of the heat fluxes to the atmosphere.

Notation

a a constant (0.003286).
a_G total albedo of the ground surface.
a_n dependence of albedo on solar zenith angle.
a_s soil albedo as a function of soil moisture.
b dimensionless soil moisture exponent (function of soil textural class).
C volumetric heat capacity.
C_i air-dry volumetric heat capacity for soil type i.
c_p specific heat at constant pressure for air.
D_η diffusivity for soil moisture.
e_s saturation vapor pressure of air.
g gravitational constant.
G soil heat flux.
h relative humidity of the surface soil.
H_s vertical sensible heat flux within the soil.
K_η hydraulic conductivity.
K_{η_s} saturation hydraulic conductivity.
k_0 von Karman's constant (0.35).
L latent heat of vaporization.
p atmospheric pressure.
P_f base 10 logarithm of the magnitude of the soil moisture potential (as a head of water, cm).
q atmospheric specific humidity.
q_G soil surface specific humidity.
q_s saturation specific humidity.
q_* turbulent specific humidity.
R_n net radiation flux at the ground.
R_v gas constant for water vapor (4.6151×10^6 erg g^{-1} K^{-1}).
t time.
T_G ground surface temperature.
T_s soil temperature.
u east-west component of velocity.
u_* turbulent velocity.
v north-south component of velocity.
W_a turbulent atmospheric moisture flux.
W_s soil moisture flux.
$(W_s)_G$ surface soil moisture flux.
z vertical coordinate within the soil.
z_0 turbulent roughness length.
Z solar zenith angle.
z_G height of ground surface above a reference level (in the soil).
δ weighting factor.
Δ fractional soil wetness.
η soil volumetric moisture content.
η_s soil porosity.
η_{wilt} permanent wilting soil moisture content (15 bar).
θ atmospheric potential temperature.
θ_* turbulent potential temperature.
λ soil thermal conductivity.
ρ air density.
ρ_w density of water
ψ soil moisture potential (as a head of water)
ψ_G surface moisture potential
ψ_s saturation moisture potential

Subscripts

G ground surface.
S saturation.
η function of soil moisture.

Acknowledgments. The authors are indebted to Roger Clapp and George Hornberger for many discussions about soil hydrology. We are also especially grateful to Robert Kessler and Mordecay Segal who painstakingly scrutinized a draft of this paper. Drafting was skillfully prepared by Steve Kempler, Neal Grandy, and Tom Adams. Blair Hawkins assisted in preparing the data. Typing was ably performed by Susan Grimstead. The numerical model was run by using the facilities of the National Center for Atmospheric Science (NCAR), Boulder, Colorado. NCAR is supported by the National Science Foundation. This research was conducted under support from a research grant from the Atmospheric Sciences Section of the National Science Foundation.

References

Al Nakshabandi, G., and H. Kohnke, Thermal conductivity and diffusivity of soils as related to moisture tension and other physical properties, *Agric. Meteorol., 2,* 271–279, 1965.

Anthes, R., and T. Warner, Development of hydrodynamic models suitable for air pollution and other mesometeorological studies, *Mon. Weather Rev., 106,* 1045–1078, 1978.

Burk, S., The moist boundary layer with a higher order turbulence closure model, *J. Atmos. Sci., 34,* 629–638, 1977.

Carpenter, K., An experimental forecast using a nonhydrostatic mesoscale model, *Q. J. R. Meteorol. Soc., 105,* 629–655, 1979.

Clapp, R., and G. Hornberger, Empirical equations for some soil hydraulic properties, *Water Resour. Res., 14,* 601–604, 1978.

Deardorff, J., Three-dimensional numerical study of the height and mean structure of a heated planetary boundary layer, *Boundary Layer Meteorol., 7,* 81–106, 1974.

Deardorff, J., Efficient prediction of ground surface temperature and moisture, with inclusion of a layer of vegetation, *J. Geophys. Res., 83,* 1889–1903, 1978.

De Vries, D., Heat transfer in soils, in *Heat and Mass Transfer in the Biosphere, I, Transfer Processes in the Plant Environment,* edited by D. De Vries and N. Afgan, pp. 5–28, Scripta, Washington, D. C., 1975.

Edlefsen, N., and A. Anderson, Thermodynamics of soil moisture, *Hilgardia, 15,* 31–299, 1943.

Gannon, P., Influence of earth surface and cloud properties on the south Florida sea breeze, *Tech. Rep. ERL 402-NHEML2,* NOAA, U.S. Dep. of Commerce, Washington, D. C., 1978.

Garrett, A., Numerical simulations of atmospheric convection over the southeastern U.S. in undisturbed conditions, *Rep. 47,* Atmos. Sci. Group, College of Eng., Univ. of Texas, Austin, 1978.

Geiger, R., *The Climate Near the Ground,* Harvard University Press, Cambridge, Mass., 1965.

Idso, S., R. Jackson, B. Kimball, and F. Nakayama, The dependence of bare soil albedo on soil water content, *J. Appl. Meteorol., 14,* 109–113, 1975.

Jadhav, G., V. Ingle, S. Varade, and K. Pawar, Moisture retention and available water capacity of Marathwada soils, *J. Indian Soc. Soil Sci., 25,* 436–438, 1977.

Lettau, H., and B. Davidson, *Exploring the Atmosphere's First Mile,* vol. I and II, Pergamon, New York, 1957.

Mahrer, Y., and R. Pielke, A numerical study of the airflow over irregular terrain, *Beit. Phys. Atmos., 50,* 98–113, 1977.

Mahrer, Y., and R. Pielke, A test of an upstream spline interpolation technique for the advective terms in a numerical mesoscale model, *Mon. Weather Rev., 106,* 818–830, 1978.

Perkey, D., A description and preliminary results from a fine-mesh model for forecasting quantitative precipitation, *Mon. Weather Rev., 104,* 1513–1526, 1976.

Petersen, G., R. Cunningham, and R. Matelski, Moisture characteristics of Pennsylvania soils, I, Moisture retention as related to texture, *Soil Sci. Soc. Am. Proc., 32,* 271–275, 1968.

Philip, J., Evaporation, and moisture and heat fields in the soil, *J. Meteorol., 14,* 354–366, 1957.

Pielke, R., A three-dimensional model of the sea breezes over south Florida, *Mon. Weather Rev., 102,* 115–139, 1974.

Rijtema, P., Soil moisture forecasting, *Note 513,* Inst. for Land and Water Manage. Res., Wageningen, The Netherlands, 1970.

Salter, P., and J. Williams, The influence of texture on the moisture characteristics of soils, II, Available-water capacity and moisture release characteristics, *J. Soil Sci., 16,* 310–317, 1965.

Sasamori, T., A numerical study of atmospheric and soil boundary layers, *J. Atmos. Sci., 27,* 1122–1137, 1970.

Sellers, W., *Physical Climatology,* University of Chicago Press, Chicago, Ill., 1965.

Tapp, M., and P. White, A non-hydrostatic mesoscale model, *Q. J. R. Meteorol. Soc., 102,* 277–296, 1976.

U.S. Department of Agriculture, Soil survey manual, *U.S. Dep. of Agric. Handbook, 18,* 1–503, 1951.

van Bavel, C., and D. Hillel, Calculating potential and actual evaporation from a bare soil surface by simulation of concurrent flow of water and heat, *Agric. Meteorol., 17,* 453–476, 1976.

Zdunkowski, W., J. Paegle, and J. Reilly, The effect of soil moisture upon the atmospheric and soil temperature near the air-soil interface, *Arch. Meteorol. Geophys. Biokl., Ser. A, 24,* 245–268, 1975.

(Received October 20, 1980;
revised May 11, 1981;
accepted July 13, 1981.)